Geomorphology 436 (2023) 108782

Contents lists available at ScienceDirect

Geomorphology

journal homepage: www.journals.elsevier.com/geomorphology

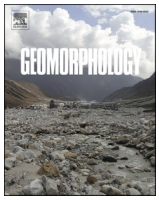

Increased erosion in a pre-Alpine region contrasts with a future decrease in precipitation and snowmelt

Tabea Cache [a,*], Jorge A. Ramirez [b], Peter Molnar [c], Virginia Ruiz-Villanueva [a], Nadav Peleg [a]

[a] Institute of Earth Surface Dynamics, University of Lausanne, Lausanne, Switzerland
[b] Department of Geography, University of Exeter, Exeter, UK
[c] Institute of Environmental Engineering, ETH Zurich, Zurich, Switzerland

ARTICLE INFO

Keywords:
Climate change impacts
Hydromorphological response
Landscape evolution
Alpine erosion
Rainfall intensification
High-resolution sediment transport

ABSTRACT

Climate change is affecting the hydromorphological system. In many places, changes in sediment dynamics are closely correlated to changes in precipitation frequency and magnitude. However, in nivo-pluvial regimes, the hydromorphological response to climate is more challenging to predict as it is not only the amount and occurrence of precipitation that is changing. The changes in precipitation type (i.e., snow or rain), snow accumulation, and snowmelt rates will also have a significant effect on the catchment net precipitation (composed of direct precipitation plus snowmelt contribution), and this may affect overland flow, erosion, stream discharge, sediment transport, and deposition. We investigated the impacts of climate change on hydrology and geomorphology in a small catchment (Emme, 127 km^2) located in the Swiss pre-Alps by simulating the difference between the hydromorphological response to net precipitation in the present climate and in three climate scenarios at the end of the century using the CAESAR-Lisflood landscape evolution model. For the most extreme climate scenario (RCP8.5), simulations showed that despite the reduction in net precipitation (by 7 %) and discharge (by 4 %), sediment yield at the outlet of the catchment increased by 6 %. This is not only because precipitation falls more as rain than snow during the cold months, but also because heavy precipitation is expected to intensify. On a seasonal scale, we found that the amount of net precipitation, discharge, and erosion will increase in winter at the end of the century, while it will decrease in spring. In all three climate scenarios, net precipitation is projected to decrease in summer, but sediment yields may both decrease or increase. Autumn is the season with the greatest changes in erosion, while net precipitation remains constant or only slightly increases. Furthermore, we found that erosion and deposition patterns are changing spatially, with more erosion in mid-elevations and more deposition in valleys. Although our results are specific to the study site, we expect similar trends in other catchments of the pre-Alpine region.

1. Introduction

Anthropogenic climate change is modifying precipitation and temperature, which are major components of the hydrological cycle and drivers of geomorphological changes (IPCC, 2022). Mountainous environments play a crucial role in water resources and sediment supply for downstream reaches (Viviroli et al., 2007) and are particularly vulnerable to climate change as they are highly sensitive to warming temperatures that affect snowfall, snow accumulation, and melt processes (Chiarle et al., 2021; Reynard et al., 2012).

Climate change directly affects runoff in mountainous catchments by affecting precipitation (rainfall and snowfall/melt) and evaporation, with precipitation being the dominant factor (Moraga et al., 2021). Globally, changes in precipitation include intensification of short-duration rainfall extremes (Ali et al., 2021b; Fowler et al., 2021; Hegerl et al., 2015; Trenberth et al., 2003) and shortening of winter periods with a shift from snow- to rain-dominated conditions (Beel et al., 2018; Huss et al., 2017; Marty, 2008; Ruiz-Villanueva et al., 2015; Scherrer et al., 2004). The hydrological response to such changes in climate in the Alpine region is likely to result in increasing winter discharge (Goudie, 2006); this can be a result of precipitation amount increasing in the future (CH2018, 2018) or of precipitation shifting from solid to liquid due to temperature increase, which will lead to more water available for surface runoff during winter (Etter et al., 2017). An

* Corresponding author.
E-mail address: tabea.cache@unil.ch (T. Cache).

https://doi.org/10.1016/j.geomorph.2023.108782
Received 1 November 2022; Received in revised form 22 May 2023; Accepted 6 June 2023
Available online 8 June 2023

increase in Alpine temperatures will lead to a significant decline in snow in the future (Beniston, 2012; Marty, 2008). In addition, spring discharges can either decrease (Moraga et al., 2021; Ruiz-Villanueva et al., 2015) or increase (Bavay et al., 2013), depending on the projected changes to spring precipitation amounts and the changes in snowmelt contribution. These changes can have a significant impact on the geomorphological response of mountainous catchments considering that snow is a major driver of upland erosion and sediment transport (Costa et al., 2018a; Iida et al., 2012; Slosson et al., 2021). On the other hand, changes in summer discharge in unglacierized mountainous catchments are seemingly not affected by snowmelt but mainly by changes in precipitation (Moraga et al., 2021). Therefore, the expected intensification of extreme summer rainfall is likely to enhance the hydromorphological response of the catchment (Peleg et al., 2020, 2022). In autumn, despite decreasing snow accumulation and thus enhanced water availability in the catchment for direct runoff, discharge is projected to decrease due to reduced autumn precipitation in Switzerland (Muelchi et al., 2021a).

Understanding how erosion and sediment transport will change with climate is crucial as sediment fluxes can threaten water quality, aquatic biota in rivers, downstream reservoirs, and infrastructure (Bilotta and Brazier, 2008; Davies-Colley and Smith, 2001; Hackney et al., 2020; Li et al., 2020). Additionally, sediment deposition can have a significant impact on flood magnitude and frequency as channel bed aggradation can reduce the conveyance capacity of the river reaches (Lane et al., 2007). A simultaneous increase in temperature, sediment production, and sediment transport has been reported in recent years for various mountainous catchments (Beel et al., 2018; Bennett et al., 2013; Costa et al., 2018a; Huggel et al., 2010, 2012; Lewis and Lamoureux, 2010; Micheletti et al., 2015). Model-based predictions of future erosion trends, however, are less in agreement. For example, Meusburger et al. (2012) project an increase in runoff erosion in Switzerland due to higher winter precipitation and a shorter winter season, yet Palazón and Navas (2016) estimate that sediment yield in a pre-Alpine catchment will decrease in a warming climate. The challenge of forecasting changes in geomorphological response in mountainous areas is not only due to the difficulty of predicting precipitation and temperature changes and their impacts but also because the catchment's physical properties may be affected as well. For example, erosion could increase on hillslopes without sediment yield changing at the outlet due to reduced connectivity between sediment sources and the fluvial system (Cavalli et al., 2013; Micheletti and Lane, 2016; Mukundan et al., 2013).

Numerical landscape evolution models (LEMs; see Section 3.5 for details) can be used to gain insight into the role of different climatic forcings on sediment and erosion processes at the catchment scale, while also taking into account changes in catchment topography and hydrological connectivity (Battista et al., 2020a, 2020b, 2022; Coulthard et al., 2012; Skinner et al., 2020). Spatially distributed LEMs are sensitive to the spatial resolution of rainfall; lumped rainfall can lead to an overprediction of sediment yield and to spatial biases of erosion and deposition (Coulthard and Skinner, 2016; Peleg et al., 2020, 2021). By combining sufficiently spatially-resolved digital elevation model (DEM) and precipitation, physically consistent LEMs allow to make robust predictions. Better insights can be gained on (a) how changes in precipitation, snow accumulation, and snowmelt can affect annual and seasonal catchment streamflow and sediment yield; (b) how intensification of precipitation might affect sediment transport at the outlet; and (c) how erosion will change across the catchment. Herein, we investigated hydromorphological changes between present and future climates in a Swiss pre-Alpine catchment using the CAESAR-Lisflood LEM and propose a new approach to include spatially varying snow processes in the model. The catchment's hydromorphological response to climate change was evaluated for three emission scenarios, representing the potential projected changes in Swiss climate at the end of the century (CH2018, 2018).

2. Study area

The impact of climate change on the hydromorphological response was investigated in the upper Emme River catchment (46.87°N, 7.79°E), Switzerland (Fig. 1). This catchment was chosen because it has (a) physical characteristics (e.g., topography and lithology, Fig. S2) and climate that are typical for pre-Alpine catchments; (b) climate and hydrology that are well monitored (Fig. S1); and (c) an appropriate area to perform numerical simulations at relatively high spatial and temporal resolutions.

The catchment drainage area is 127 km^2 and elevations are between 744 and 2205 m a.s.l. The climate is temperate, with an average temperature ranging from −5 °C in January to 13 °C in July, and a mean annual areal precipitation of 1764 mm. The glacier-free catchment is mostly covered by agricultural land (50 %) and less than 10 % is urbanized. The flow regime is not affected by reservoirs or dams and there is no major water withdrawal.

3. Method and data

Fig. 2 summarizes the numerical approach used in our study. First, the climate data representing the present (1981–2010) and future (2071–2100) climates were generated at hourly resolution, under three emission scenarios. Second, the generated climate data were downscaled and used to drive a snow accumulation and snowmelt model at hourly and 100 m resolutions. Third, outputs from the snow model served as input into the CAESAR-Lisflood LEM which simulated scenarios of hydromorphological change at 50 m resolution in the catchment. Lastly, using the CAESAR-Lisflood outputs, the hydromorphological responses (sediment transport, erosion, and deposition) were evaluated at the catchment outlet and within the catchment.

3.1. Present climate

Five climate stations, operated by MeteoSwiss, are located between 6 km and 13 km from the catchment boundary (Fig. S1). Station hourly precipitation, near-surface air temperature at 2 m (hereinafter referred to as temperature), and near-surface wind speed at 10 m were obtained for the period between 2016 and 2020. Since observed data for all stations are only available from 2016, the natural stochastic variability of

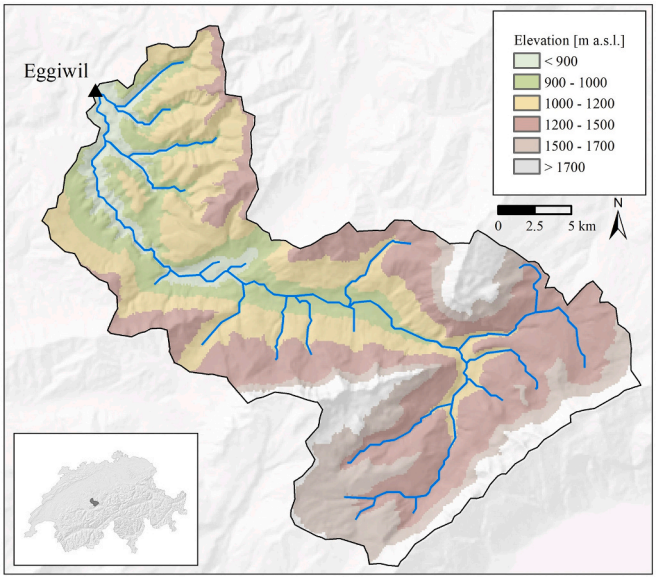

Fig. 1. Hillshade, elevation and location in Switzerland of the upper Emme River catchment.

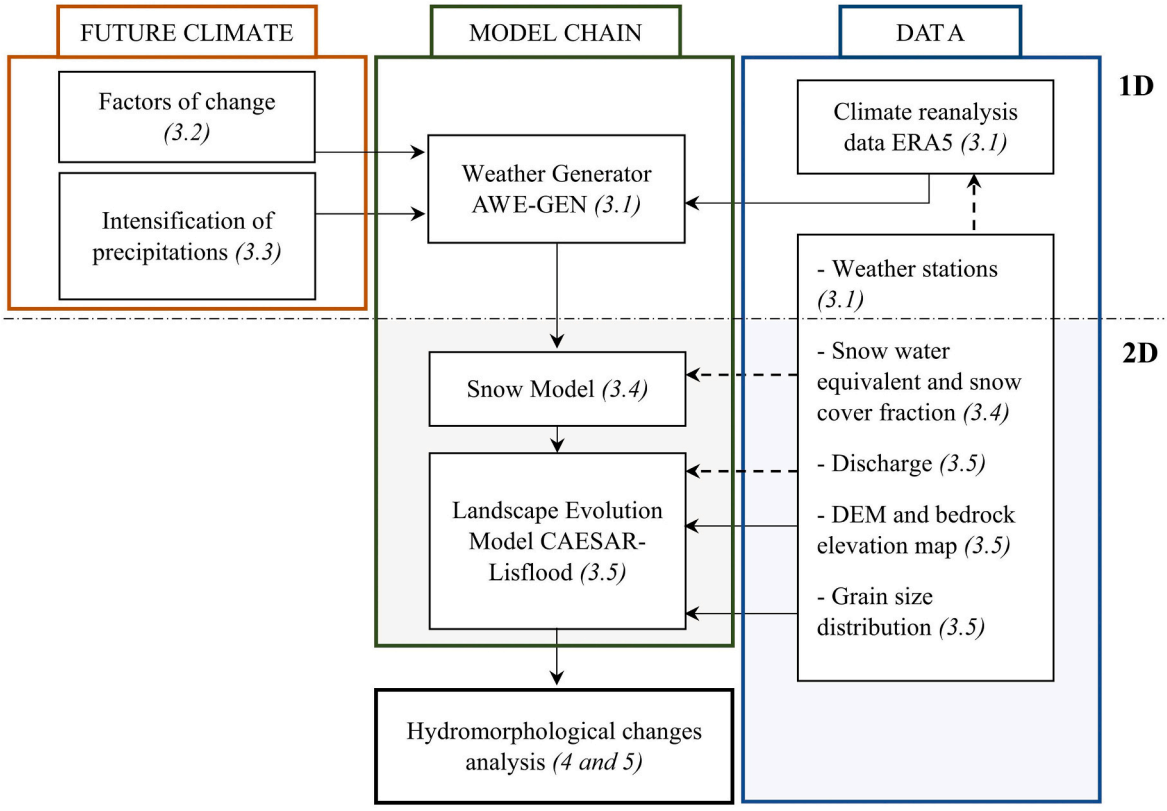

Fig. 2. Schematic overview of the methodology. Refer to the section numbers in brackets for further information. Dashed arrows indicate data used for bias correction, calibration, or validation.

climate is not represented (30 years of data are recommended, see WMO, 2018). Therefore, we used data from a climate reanalysis product as our reference for the present climate (Alves et al., 2021; Hersbach et al., 2020). The ERA5 reanalysis product (Hersbach et al., 2018) has hourly climate data that is uninterrupted from 1950 to present and is the optimal reanalysis product for this region (Horton, 2021). We extracted from ERA5 the same climate variables as obtained from the climate stations for the period 1981–2010.

Climate reanalysis is known to contain biases and often requires a bias correction to agree with ground observations (Cucchi et al., 2020; Yin et al., 2021). The bias correction involved two adjustments to precipitation: removing precipitation below a certain threshold to correct the frequency and applying a quantile mapping to correct the intensities (Piani et al., 2010). Both corrections were applied separately for each month to preserve the seasonality of precipitation frequency and intensity. The correction parameters were determined on the observed and ERA5 data from 2016 to 2020 and applied to ERA5 data from 1981 to 2010 assuming that both precipitation frequency and intensity are stationary between the two periods. The bias-corrected ERA5 data for 1981–2010 were then used to calibrate the AWE-GEN weather generator and to simulate present climate hourly precipitation, temperature, and wind time series. The AWE-GEN model generates climate data with the same statistical properties as the data used for calibration; the ERA5 data in this case. The AWE-GEN model has successfully been applied in many climate change studies (e.g., Fatichi et al., 2016, 2021) as well as in geomorphic studies (e.g., Hirschberg et al., 2021). The reader can refer to Fatichi et al. (2011) for a complete description of the model.

The hourly uniform precipitation time series generated by the AWE-GEN model were transformed to spatially varying rainfall fields with 100 m grid cell resolution using a simplified version of the STREAP model (Paschalis et al., 2013). The model has been applied many times in the Swiss region (e.g., Peleg et al., 2022). A concise summary of the model is provided here but the reader can refer to Paschalis et al. (2013) for further details. Precipitation fields in space and time were modeled by first generating stochastic Gaussian quantile fields using computationally efficient algorithms of the fast Fourier transform. The temporal correlation of the precipitation fields was modeled through an autoregressive moving average process and controlled by wind speed and direction. The normalized quantile fields were then converted to precipitation fields using an inverse lognormal distribution and monthly spatial coefficient of variation that were derived from calibration for a neighboring location (K. Emme catchment; Peleg et al., 2020).

Besides precipitation, we also required the temperature to be a gridded product as it is a crucial factor to distinguish between precipitation falling in liquid or solid form. Temperature, which is elevation-dependent, was initially generated for a reference elevation. By introducing a lapse rate parameter (*lr*) that defines the rate at which temperature decreases as elevation increases, the temperature was calculated for all elevations in the catchment (e.g., Ragettli and Pellicciotti, 2012). The calibration of the lapse rate is explained in Section 3.4.

3.2. Future climate

Climate model outputs allow estimating Factors of Change (FC) that can be combined with the present climate to generate time series of the required climate variables for a future period (Fatichi et al., 2011; Moraga et al., 2021; Peleg et al., 2019). FC can describe either additive (e.g., for temperature) or multiplicative (e.g., for precipitation) differences between statistics of baseline and future climate variables. Three Representative Concentration Pathways (RCP; IPCC, 2022) were considered when computing FC: a stringent mitigation scenario (RCP2.6), an intermediate scenario (RCP4.5), and an unmitigated scenario (RCP8.5). The median FC from the official Swiss climate projections (CH2018, 2018) for mean precipitation and temperature were used as an input into the AWE-GEN model on a seasonal basis to generate plausible future climate variables over the period 2071–2100

with respect to the 1981–2010 reference period. AWE-GEN stochastically generates each 30-year realization independently to address the natural climate variability (Fatichi et al., 2016), keeping the FC of mean temperature and precipitation (Table 1, Table S2) in general agreement with the CH2018 FC.

3.3. Rainfall intensification

Using FC on mean statistics to simulate future climate is a simple method, yet it has limitations in hydromorphological impact studies (Coulthard et al., 2012). The main limitation is linked to its inability to explicitly modify low- and high-frequency events (Moraga et al., 2021), which will underestimate the expected intensification of extreme rainfall in all seasons across Switzerland (CH2018, 2018.; IPCC, 2022), and hence the expected hydromorphological response (Costa et al., 2018b; Micheletti and Lane, 2016).

The estimated intensification of short-duration extreme rainfall intensity in Switzerland has a rate of 6–13 % $°C^{-1}$ (Molnar et al., 2015), which is close to the theoretical Clausius-Clapeyron intensification rate of 7 % $°C^{-1}$ (Trenberth et al., 2003), and to the global estimate (Ali et al., 2021a). We computed the scaling of hourly extreme rainfall with temperature by applying the binning method to the observed temperature and rainfall in the catchment (Lenderink and Van Meijgaard, 2008). Intensification rates were computed for the 90th to 99.9th percentile hourly rainfall using 12 equally sized temperature bins and a linear regression from the bin with lowest to highest temperature (limiting the analysis to temperatures exceeding 5 °C to avoid snow events; Ali et al., 2021a). The scaling rates are higher as precipitation intensity increases; the intensification rates computed for the 90th, 99th and 99.9th percentiles are respectively 5.2 % $°C^{-1}$, 8.1 % $°C^{-1}$ and 10.6 % $°C^{-1}$. Extreme rainfall generated by the AWE-GEN model was intensified post-simulation considering the observed scaling rates and the predicted increase in temperature. We kept the seasonal total volumes of simulated precipitation unchanged by lowering all precipitation intensities to compensate for the increase in intense rainfall.

3.4. Snow module

The catchment is located in the pre-Alps where snow processes play an important role in the hydrological system (Muelchi et al., 2021b). However, in its original version, precipitation is the only input to the CAESAR-Lisflood model. Using precipitation without pre-processing would imply that snow is directly routed in the model (i.e., snow accumulation and melt are ignored). To overcome this issue, precipitation was pre-processed before being used as input (Bennett et al., 2014; Welsh et al., 2009). The pre-processing involved partitioning of precipitation between rain and snow, snow accumulation and eventually melting of the snowpack. The sum of precipitation falling in liquid form and snowmelt is referred to as "net precipitation" and constituted the input to CAESAR-Lisflood.

The first step of the snow module is the partitioning of precipitation into rain or snow based on a snowfall temperature threshold (P_T). All precipitations were considered to fall either in solid or liquid form if the temperature is respectively below or above the snowfall temperature threshold. Snowpack accumulation and melting were simulated using the Enhanced Temperature Index model (ETI; Carenzo et al., 2009) where the snow albedo is expressed as a logarithmic decay of fresh snow albedo (Brock et al., 2000):

$$M = \begin{cases} TF \times T + SRF \times (1-\alpha) \times I, & T > T_T \\ 0, & T \leq T_T \end{cases} \quad (1)$$

where T is the hourly temperature, I is the incoming shortwave radiation, T_T is the melt onset temperature threshold, TF and SRF are temperature and shortwave radiation parameters, and α is the albedo that is expressed as:

$$\alpha = \alpha_1 - \alpha_2 log_{10}(T_{acc}) \quad (2)$$

where α_1 and α_2 are respectively the fresh snow albedo and the empirical snow albedo parameter and T_{acc} is the accumulated daily maximum temperatures since the last snowfall.

Most of the parameters can be fixed as constants from literature for similar Alpine sites: $TF = 0.04$ mm d^{-1} $°C^{-1}$, $SRF = 0.0105$ m^2 mm W^{-2} h^{-1}, $\alpha_1 = 0.713$ and $\alpha_2 = 0.07$ (Brock et al., 2000; Carenzo et al., 2009; Ragettli and Pellicciotti, 2012). The temperature lapse rate (lr), the snowfall temperature threshold (P_T), and the melt onset temperature threshold (T_T) were calibrated with snow water equivalent (SWE) data measured by the Swiss Federal Institute for Forest, Snow and Landscape Research (WSL) for the period 1999–2015. The following parameters were calibrated based on the monthly mean SWE averaged over the study area with a Nash-Sutcliffe Efficiency (NSE, ranging from $-\infty$ to 1, where 1 is the optimal value; Nash and Sutcliffe, 1970) of 0.93: lr = 7.5 °C km^{-1}, $P_T = -1$ °C and $T_T = 5$ °C.

Simulated snow cover extent was validated by comparing the annual duration of snow-covered cells in seven different elevation bands with the satellite imagery snow-cover product MODIS MOD10A1 (Costa et al., 2018b; Hall and Riggs, 2021; Fig. S3) for the years 2000 and 2001. MODIS cells may not be classified as snow cover in case of missing data or cloud cover for example. Therefore, images with more than 30 % of the cell information not classified as snow cover were excluded from the analysis (Costa et al., 2018b). Cells were accounted as snow-covered if the simulated snow depth was larger than 1 cm (Stanzel et al., 2008). The validation was conducted by dividing the catchment into seven different elevation bands to account for the spatial variability of snow accumulation.

3.5. CAESAR-Lisflood LEM

CAESAR-Lisflood (Coulthard et al., 2013) is a LEM that simulates erosion and deposition at high space-time resolution within catchments (e.g., Hoober et al., 2017) and river reaches (Feeney et al., 2020; Poeppl et al., 2019; Ramirez et al., 2020; Ziliani et al., 2020). The model is a combination of the Lisflood-FP 2D hydrodynamic model that generates the flow propagation (Bates et al., 2010) and the CAESAR cellular automaton geomorphic model (Coulthard et al., 2002; Van de Wiel et al., 2007). In CAESAR-Lisflood, rainfall-runoff is estimated using a modified version of TOPMODEL (Beven and Kirkby, 1979) and a simplified form of the shallow water equations to compute discharge across cell boundaries in each cardinal direction. Manning's equation is then used to calculate flow depth and velocity, which are used to derive shear stress. The CAESAR-Lisflood model does not distinguish between overland flow and streamflow which are simulated in the same manner. The simulated shear stress is then used to estimate sediment erosion from each cell using the Meyer-Peter and Müller (1948), Wilcock and Crowe (2003), or Einstein (1950) sediment transport formulae. Bedload sediments are deposited in neighboring cells, while suspended sediments deposit according to sediment fall velocity and concentration. Up to 9

Table 1
Seasonal FC for temperature (additive) and precipitation (%) between the simulated 1981–2010 reference period and the 2071–2100 future climates for RCP2.6, RCP4.5, and RCP8.5.

	DJF	MAM	JJA	SON
Mean change in temperature [°C]				
RCP2.6	0.94	1.91	1.30	1.11
RCP4.5	2.24	2.09	3.17	2.31
RCP8.5	3.57	3.90	5.46	4.26
Mean change in precipitation [%]				
RCP2.6	11.4	−1.8	−0.4	−11.1
RCP4.5	−1.9	−0.1	−4.1	−1.3
RCP8.5	6.9	0.6	−19.7	−7.9

sediment grain sizes can be modeled, with three having the option of being bedload or suspended. Importantly, modeling multiple grain sizes allows for the representation of spatially varying grain size distribution. In each cell of the DEM, grain sizes are stored in a surface active layer, several buried layers (strata), and a base layer. All these layers are underlaid by a bedrock layer which can either be set as erodible or non-erodible across the entire study area. Slope processes, such as landslides and soil creep, are modeled as a function of user-defined constant thresholds or rates to allow material to be transported from the hillslopes into the channels. As such, slope failures do not consider soil saturation. For a full description of CAESAR-Lisflood, the reader can refer to Coulthard et al. (2013).

The precipitation input can be distributed (e.g., Peleg et al., 2021), making CAESAR-Lisflood ideal to study the impact of a changing climate where snow processes vary spatially. In addition, CAESAR-Lisflood has been frequently applied in Alpine landscapes (Peleg et al., 2020; Ramirez et al., 2020, 2022; Welsh et al., 2009) and this provides further support for using the model in the current study.

The catchment topography was represented in the model using a DEM (Fig. 1), and a bedrock elevation map was used to determine the depth of erodible sediments (Fig. S1). Both datasets were obtained from the Swiss Federal Office of Topography (swisstopo), at a grid resolution of 50 m. The sediment grain size distribution (with six-grain sizes, Table 2) was measured at three locations in the catchment and assumed to be representative of the entire catchment (Baudirektion des Kantons Bern, 1988; Fig. 1; Section S1; Fig. S4). Most of the hydrological, hydraulic, and geomorphic parameters for CAESAR-Lisflood were adopted from a study in the Kleine Emme, an adjacent catchment to the upper Emme River catchment (Peleg et al., 2020), and are listed and explained in Table S1. Three CAESAR-Lisflood parameters were calibrated (Fig. S5) to adapt the model to this study: (1) the discharge threshold for depth calculation Q_{min} (below this threshold, the sediment flux is assumed to be negligible and the hydrodynamic model is allowed to run in a steady state to speed up computations); (2) the Manning's n roughness coefficient; and (3) the m value (this parameter controls the duration and peak of the hydrographs generated by rainfall events). The model parameters were kept constant throughout all simulations. As the grain sizes are initially homogeneously distributed in the catchment, a 10-year spin-up simulation was run to generate a more representative spatial distribution of grain sizes across the catchment (Coulthard and Skinner, 2016; Skinner et al., 2020).

We validated the hydrodynamics of CAESAR-Lisflood by comparing the simulated and observed hydrograph at the outlet of the catchment for an intense precipitation and discharge event that occurred on August 30th, 2017. We chose this event because it has good meteorological and discharge data. Additionally, the discharge is not influenced by antecedent hydrological conditions as it was close to baseflow before the start of the event. The observed discharge at the outlet (Eggiwil; Fig. 3) was recorded by the Swiss Federal Office for the Environment at intervals of 1 h. Besides an adequate NSE value of 0.82, the maximum absolute error (MaAE) is as low as 3.87 $m^3\ s^{-1}$. This implies that the model can satisfactorily simulate the intense hydrological response of the catchment.

Because of the absence of monitored sediment yield in the catchment, the sediment yield simulated by CAESAR-Lisflood can only be validated with erosion rates in similar environments. For the present climate (1981–2010), the simulated mean annual sediment yield at the outlet of the catchment was $275.5 \times 10^3\ m^3\ yr^{-1}$. Assuming a mean sediment density of 2 Mg m^{-3} (Zappone and Kissling, 2021), the mean annual sediment yield can be converted to 4300 Mg $km^{-2}\ yr^{-1}$. This value agrees with erosion rates reported in the literature for catchments of similar size (García-Ruiz et al., 2015). Additionally, the simulated suspended sediment concentrations are in agreement with observations in a similar river in the neighboring Kleine Emme catchment (Battista et al., 2020a; Section S2 and Fig. S6).

Table 2
Particle size distribution and contribution to sediment yield (SY) at the outlet in the simulation for present climate.

Grain size [mm]	Proportion in the river channel [%]	Contribution to baseline SY [%]
0.4	3.5	16.1
10	14.5	43.3
40	20.3	27.8
100	24.5	7.8
200	25.0	3.7
500	12.2	1.3

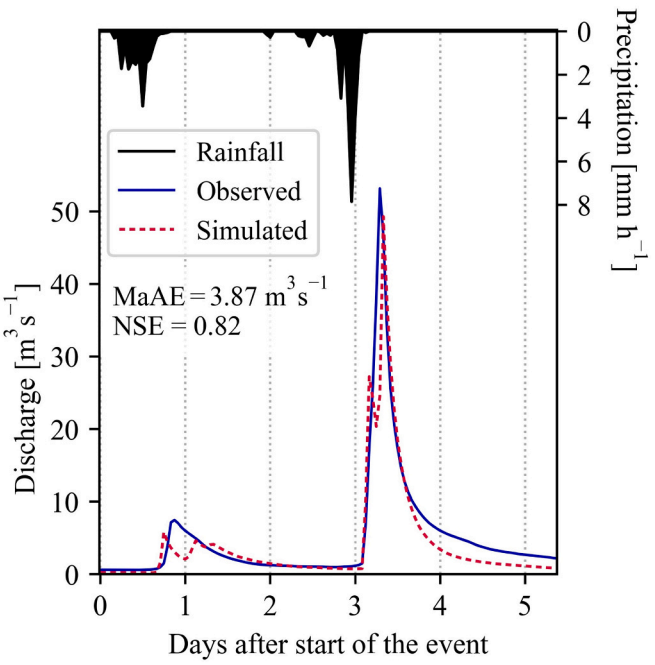

Fig. 3. Observed and simulated discharges at the outlet of the catchment for the validation event with Q_{min} = 0.03 $m^3\ s^{-1}$, n = 0.08, and m = 0.005.

4. Results

We first present the results of the changes in climate and their hydromorphological response at the outlet of the catchment for seasonal scales and individual extreme events. We then present the impact of climate change on erosion and deposition across the catchment.

4.1. Climate change

We found that the seasonal changes in net precipitation at the end of the century were more pronounced in RCP8.5 than in RCP2.6 (Fig. 4), as expected. In RCP2.6, winter was the only season for which the difference from the present climate was higher than 10 %, i.e., likely higher than the natural climate variability (Fatichi et al., 2016). In RCP4.5 and RCP8.5, the 10 % threshold was exceeded also for the spring period, and in RCP8.5 also for the summer period.

Winter was the season with the highest changes to net precipitation in all three emission scenarios (Fig. 4), even though the precipitation amount itself was small. This was due to an increase in precipitation introduced by the FC (Table 1) but also by the warming climate increasing snowmelt by 39 %, 66 %, and 101 % in RCP2.6, RCP4.5, and RCP8.5, respectively. While snowmelt increased in all three scenarios, this is not the case for snowfall which decreased by more than 20 % in RCP4.5 and RCP8.5 but increased by 4 % in RCP2.6. The increased winter precipitation in RCP2.6 thus compensated for the 0.94 °C warmer winter leading to the increase in snowfall. The reduced snow

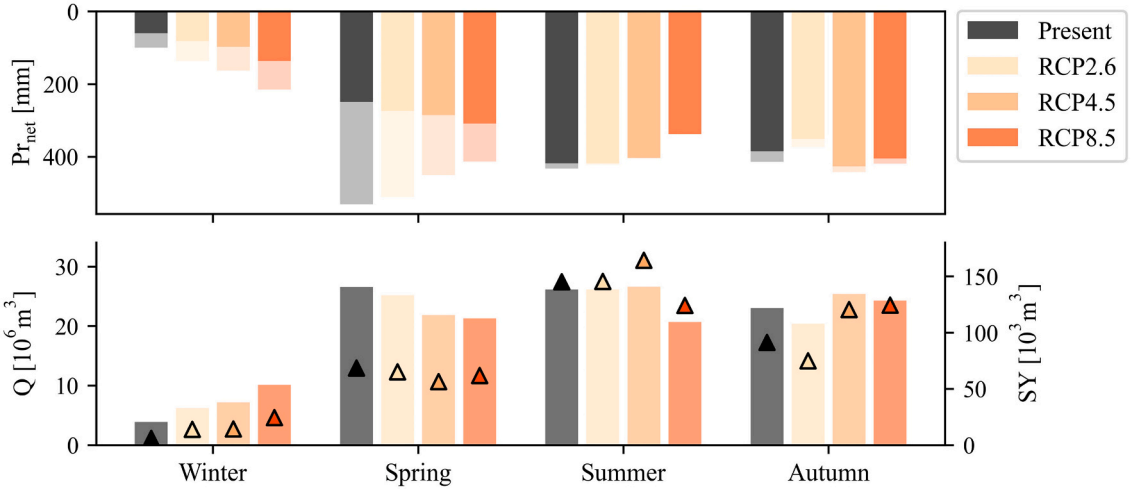

Fig. 4. Total seasonal net precipitation (Pr_{net}, bars of rainfall and snowmelt - respectively without and with transparency), discharge (Q, bars) and sediment yield (SY, triangles) at the outlet of the catchment for the present (grey-black) and the three climate scenarios (yellow to orange) representing the climate at the end of the century.

accumulation in winter impacted the net precipitation in spring. This is due to lower snow availability for melting and thus less snowmelt, which is an important contributor to net precipitation in spring. Consequently, despite the negligible FC for spring precipitation (with changes up to 1.8 % only), the net precipitation was reduced for all the RCPs, with a maximum reduction of 22 % for RCP8.5.

In summer, the snow processes were negligible as net precipitation consisted of 97 % of rain in the present climate and more than 99 % in the future. On one hand, summer precipitation amounts were decreasing, especially in RCP8.5 where the reduction reached 20 % (Table 1), but on the other hand, summer extreme rainfall was intensifying due to warmer temperatures. Net precipitation in autumn did not change considerably (maximum change of 7.1 %, Fig. 4). Despite a precipitation reduction in all future scenarios (Table 1), net precipitation increased in RCP4.5 and RCP8.5. The major change was the decrease of snowfall by more than 34 %, which led to a decrease in snowmelt by more than 26 % due to a lower snow cover.

4.2. Discharge at the outlet

The changes to net precipitation were reflected in the discharge. As a result, the hydrological response in RCP2.6 was similar to the present climate while the response was greatly impacted in RCP8.5 (Fig. 4). Due to the small runoff in winter, future winters were found to have the greatest proportional seasonal difference compared to the present discharge. However, the highest absolute differences were found in autumn for RCP2.6, in spring for RCP4.5, and in summer for RCP8.5.

Discharges increased in winter by 60 %, 85 %, and 161 %, and decreased in spring by 5 %, 18 %, and 20 % for RCP2.6, RCP4.5, and RCP8.5, respectively (Fig. 4). The lack of snow dominated the changes in spring, especially for RCP4.5 as the FC between RCP4.5 and the baseline scenario in spring was only −0.6 % for precipitation and reached 18 % for discharge. While the total discharge in summer was reduced in RCP8.5 by 21 %, which is similar to the change in net precipitation, RCP2.6 and RCP4.5 summer discharges remained similar to the present (maximum change of 2 %) due to only a small decrease in summer precipitation. In autumn, discharges decreased in RCP2.6 and increased in RCP4.5 and RCP8.5 due to the higher proportion of precipitation falling in liquid form (Fig. 4).

In all simulations, seasons with equal total net precipitation might not lead to equal total discharge. For example, although net precipitation in spring was higher than in summer in RCP2.6 and RCP4.5, total discharge in summer exceeded that in spring. Seasons with more intense hourly net precipitation yet less total precipitation had higher mean seasonal discharge (Fig. S7). This agrees with the non-linear response of discharge to precipitation reported in previous studies (Coulthard et al., 2012). In RCP8.5, however, the intensification of hourly summer rainfall did not compensate for the seasonal reduction of precipitation amount.

4.3. Sediment yield at the outlet

In the present climate, the seasonality was marked by high sediment yield in summer and almost no sediment yield in winter (Fig. 4). This was still the case for RCP2.6 and RCP4.5 but less for RCP8.5 where autumn sediment yield increased compared to the present climate, making it the season with the highest sediment yield. In RCP4.5, the sediment yield in autumn increased too, but summer was still the season with the highest sediment yield (Fig. 4). In all future climate simulations, sediment yield at the outlet increased in winter and decreased in spring.

Despite the negligible proportion and volume of suspended sediments (defined as grain size 0.4 mm in the model) compared to the other grain sizes, the suspended sediments were relatively large contributors to the total sediment yield at the outlet due to their easy mobilization (Table 2). The impact of the grain size is also illustrated by the fraction of sediment yield for 40 mm and 100 mm; the proportion in the catchment of the former was larger than the latter, yet sediments with smaller grain sizes were more eroded and transported towards the outlet (Table 2). The contribution of the different grain sizes to total sediment yield at the outlet did not change at the end of the century (Table S3).

4.4. Climate-hydrology-geomorphic multiplier

A complex non-linear relation between net precipitation, discharge, and sediment erosion and transport was observed in the model. For example, in RCP8.5, similar spring and summer net precipitations and discharges led to different sediment yields and different summer and autumn discharges led to similar sediment yields (Fig. 4). This nonlinearity was also observed when comparing the total volumes of precipitation, discharge, and sediment yield (Table 3). In comparison to the present climate, the future climate was drier (RCP4.5 and RCP8.5) and the discharge remained either in the same order (RCP4.5) or decreased (RCP8.5) but the total sediment yield increased.

The contribution of hourly sediment yields to total sediment yield at the outlet was also analyzed according to their percentile volume. More than 90 % of the total sediment yield at the outlet was a result of the 10

Table 3
Percent of total precipitation, discharge, and sediment yield at the outlet in future scenarios compared to the baseline scenario.

	Precipitation (%)	Discharge (%)	Sediment (%)
RCP2.6	99	100	100
RCP4.5	98	101	113
RCP8.5	93	96	106

% largest hourly sediment yields for both baseline and RCP8.5 (Fig. 5); most sediments that were transported out of the catchment were flushed during high flows. In fact, the average discharges causing these hourly sediment yields were 14.2 $m^3 s^{-1}$ and 15.1 $m^3 s^{-1}$ for the present and RCP8.5 simulations respectively, corresponding to the 3 % highest hourly discharges. The ratio between the mean discharges and the cumulative volume of hourly sediment yields belonging to different percentile classes highlighted the amplification effect from discharge to sediment. In fact, the cumulative volume of the 90th to 100th percentiles hourly sediment yields was around 20 times higher than the cumulative volume of the 80th to 90th percentiles. This ratio reduced to 5 when comparing the mean discharges simulated simultaneously to these sediment yields.

4.5. Erosion and deposition across the catchment

We further analyzed the differences between the DEMs after running 30-year simulations for present and RCP8.5 (Fig. 6). As end-of-simulation DEMs include changes from the initial DEM, the analysis of the difference between two (or more) end-of-simulation DEMs is not straightforward. A negative difference between RCP8.5 and baseline end of simulation DEMs can correspond either to a decrease in deposition or an increase in erosion in future climate compared to present (Fig. 6a). Positive DEM differences were concentrated in low elevations and absent in high elevations (above 1000 m). In higher elevations, erosion increased in future climate compared to the baseline simulation. However, erosion was limited at elevations higher than 1500 m (Fig. 6b) where depth to bedrock is lower or even null (Fig. S1). Additionally, grid cells located in low elevations mostly eroded in the present climate and RCP2.6, while experiencing deposition in RCP4.5 and RCP8.5 (Fig. 6b), showing the shift from erosion- to deposition-dominated valleys in the future. This might be due to higher erosion on slopes and a limited transport capacity downstream. Fig. 6 also shows that cells with negative values were sparser than the positive ones: unlike deposition, the increase in erosion was not mainly concentrated along rivers.

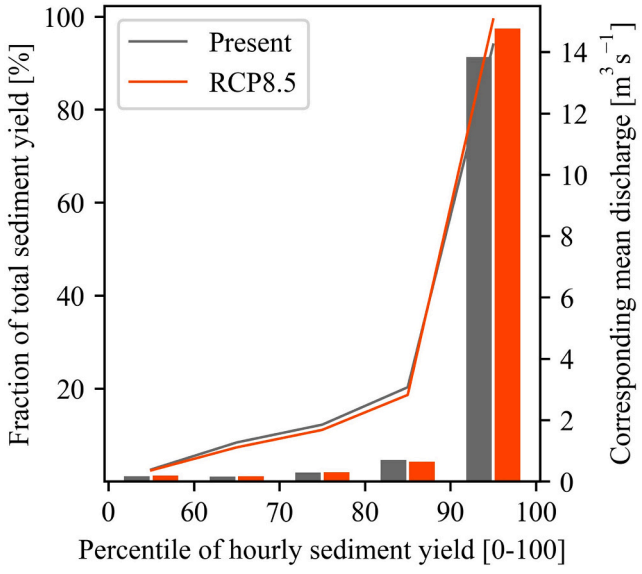

Fig. 5. Fraction of total sediment yield at the outlet for different percentiles of hourly sediment yields in the baseline and RCP8.5 scenarios (bars) along with the corresponding simulated mean discharges (lines). RCP8.5 hourly sediment yields are classified according to the hourly sediment yield volume threshold corresponding to present climate percentiles.

The monthly total erosion of suspended and d50 sediments (0.4 mm and 100 mm, respectively) across the catchment is analyzed against monthly precipitation (Fig. 7). There was considerably more data for monthly net precipitations below 10 mm at present compared to RCP8.5 since winter solid precipitation accumulated more in the present colder climate. As solid precipitation accumulates in present cold months, the net precipitation is low compared to future warmer months where solid precipitation melts and contributes to net precipitation. The linear fits for both grain size sediments have a steeper slope for the RCP8.5 simulation data than for the baseline ones (Fig. 7, Table S4). This implies that in RCP8.5 climate conditions, we can expect more erosion to occur than in the present climate in wet months, i.e., months with more than 60 mm of precipitation. Furthermore, the months with the highest erosion corresponded to months where snow accumulation was negligible, i.e., the warm summer months where short-duration rainfall events intensified. Considering the non-linear response of hydromorphology to precipitation and the role of high-intensity discharge events in sediment transport (Sections 4.4 and 4.5), it is expected that months with equal net precipitation but with different distributions of rainfall intensities will experience different erosion rates.

5. Discussion

Our results showed that for the study site, climate change impacts non-linearly the relation between net precipitation, streamflow, and sediment yield (Table 3, Fig. 5), in agreement with previous studies (Coulthard et al., 2012; Skinner et al., 2020). Moreover, the changes were amplified under RCP8.5 compared to RCP2.6 and RCP4.5 (Table 3), as also reported for other pre-Alpine catchments (Muelchi et al., 2021b). Seasonally, the magnitude and direction of the impact were not the same (Figs. 4 and 7). An increase in winter discharge and sediment yield accompanied by a decrease in spring was found in all future simulations. This is a result of the precipitation shift from snow to rain allowing precipitation to contribute to runoff earlier as it is not stored in the snowpack and leads to discharge becoming more evenly distributed through the seasons towards the end of the century. While some studies have suggested a possible disappearance of snow in foothill regions around the Alpine chains by the end of the century (Beniston, 2012), we found that this is not the case in our pre-Alpine catchment. Additionally, total sediment fluxes are found to be more susceptible to climate change than discharge, which is a similar result to previous studies (Lewis and Lamoureux, 2010; Li et al., 2020). The impact of the shift from nivo-pluvial towards pluvial regimes on discharge seasonality agrees with studies in similar catchments (Meißl et al., 2017; Moraga et al., 2021) yet it contrasts with results for mountain catchments with runoff projected to increase also in spring (Bavay et al., 2013; Slosson et al., 2021).

Our finding that high sediment yield events are the main contributor to total sediment yield (Fig. 5) has also been observed in other catchments (Costa et al., 2018a; Coulthard et al., 2012; Micheletti and Lane, 2016). We stress that in warm seasons the amplification effect from precipitation to discharge and from discharge to sediment yield for high-intensity rainfall events resulted in an increase in total sediment yield despite the decrease in total precipitation in future climates (Table 3, Fig. 4). This is a result of the intensification of heavy rainfall due to increased water holding capacity of the air (Fowler et al., 2021) and agrees with our finding that for similar monthly net precipitation, higher erosion is expected under future climate condition compared to present climate (Fig. 7). In cold seasons, the shift from a nivo-pluvial towards a pluvial catchment led to an average three times higher change in sediment yield than net precipitation, as winter precipitation was falling

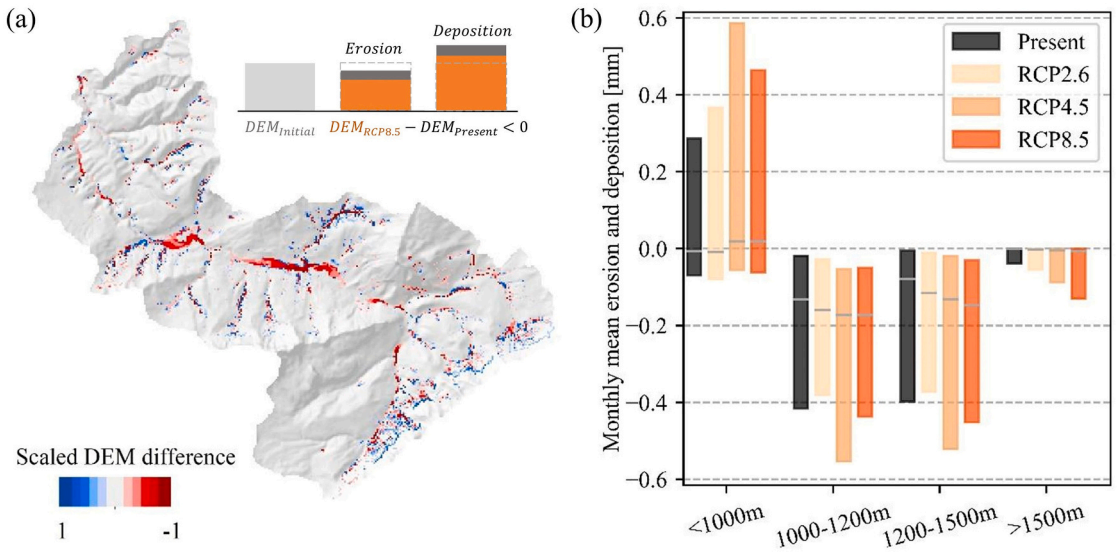

Fig. 6. (a) Scaled difference between the end of simulation DEMs for RCP8.5 and present. (b) Boxplot of monthly mean erosion and deposition for different elevation ranges (refer to Fig. 1). Boxes range from 25th to 75th percentiles and the horizontal grey lines indicate the median values. Negative and positive values correspond respectively to erosion and deposition.

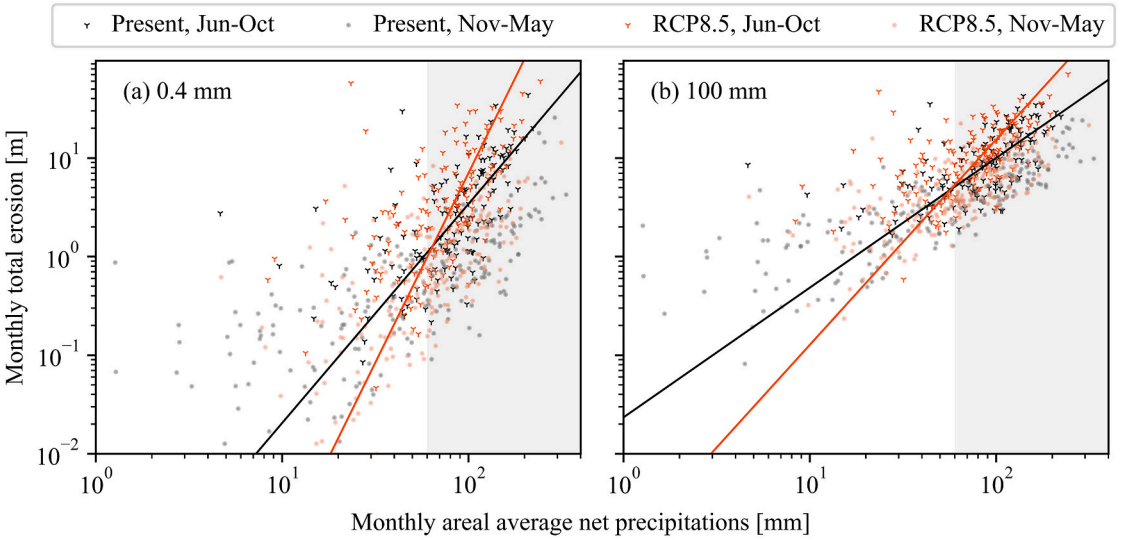

Fig. 7. Log-log plot of monthly total erosion in the catchment as a function of monthly areal average net precipitation for the present climate and RCP8.5 simulations for (a) 0.4 mm (suspended sediments) and (b) 100 mm (d50) grain sizes. Black (present) and orange (RCP8.5) lines are linear fits. The shaded areas show what is referred to as wet months in the text.

increasingly as rainfall. As similar trends in the intensification of summer heavy rainfall and the shift towards a pluvial catchment system in winter are foreseen along the Alps (Molnar et al., 2015; Moraga et al., 2021), we expect the same mechanism observed in our catchment to be applied to other pre-Alpine catchments. However, the contribution of the different grain sizes to sediment yield at the outlet remained unchanged between present and future climates.

We have tested the significance of the trends reported in the results section using the Mann-Whitney *U* test (Mann and Whitney, 1947) for a significance threshold of 0.05. We note that the trend in sediment yields at the outlet of the catchment is not statistically significant in RCP8.5 despite the decrease in net precipitations being significant (Table 3). In RCP4.5, the decrease in net precipitation is not statistically significant, while the increase in sediment yield is significant, and in RCP2.6, neither changes are significant. Despite the trend in sediment yield not being statistically significant in RCP8.5, we stress that the changes are beyond the model's expected uncertainties (Skinner et al., 2018), and that mean changes at the outlet provide only partial information. However, considering the significance of the trends across the catchment, we found that the changes in monthly mean erosion and deposition (Fig. 6) are significant for RCP4.5 and RCP8.5 in all elevation bands. Additionally, the trends in mean annual sediment yields dampen the changes in high sediment yields (90th percentile), for which the changes are statistically significant in all the emission scenarios.

We also show that the impacts of climate change on erosion and deposition differ across the catchment, with erosion increasing in high elevations and decreasing in the valleys (Fig. 6). Similar trends are reported by Hirschberg et al. (2021) for a nearby Alpine catchment. Snowpack melting and precipitation partitioning between snow and rainfall depend on temperature, and therefore high elevations (where snow processes are more meaningful) are more sensitive to changes in net precipitation. The catchment's hypsometry is thus an important

characteristic that modulates changes to future net precipitation and subsequently to sediment transport (Slosson et al., 2021). This highlights the need to use a distributed and relatively high spatial resolution LEM that can also explicitly account for different precipitation types when assessing changes to the hydromorphological response in mountainous catchments.

We analyzed the geomorphological changes between the present and future climates by running a 30-year simulation for each scenario. However, CAESAR-Lisflood has a simplified framework for modeling vegetation which is not representative in the context of climate change. Vegetation interaction with erosion was therefore not represented in the model, although climate warming can involve biomass changes (e.g., Fatichi et al., 2021) that could significantly impact sediment transport (Gianinetto et al., 2020; Palazón and Navas, 2016). Other processes were not represented such as snow gliding, reduced precipitation erosivity through snow accumulation, or the impact of the bedrock geology on erosion (Geitner et al., 2021; Meusburger et al., 2014). The changes to slope failures were not investigated as their representation in CAESAR-Lisflood is simplistic, with no consideration of soil saturation. Future development of the model including a more physically-based way of modeling landslides should be addressed in future research. Furthermore, the LEM simulated a constant evaporation rate, independent of temperature. However, evapotranspiration will increase in a warming climate which will reduce the runoff and could potentially impact the geomorphological response (Mukundan et al., 2013). Yet, excluding some processes in similar modeling frameworks (Battista et al., 2020a, 2022) allows to isolate the effects of the different sediment erosion and sediment transport drivers. Future climate change impact studies are suggested, therefore, to explicitly consider the effects of climate change on both sediment supply and sediment transport. Here, the latter was investigated in response to changes in precipitation.

Beyond the processes that were not represented in the model, we also note that the sediment yield was not validated specifically for this catchment and for the specific simulated years. Despite several surveys having been conducted in the catchment, no continuous monitoring measurements are available. We therefore only compared the simulated estimates to observations from other catchments (see Section 3.5); this approach is a common one in LEM modeling (e.g., Coulthard et al., 2012; Coulthard and Skinner, 2016). The simulated erosion rate is higher than other values reported for Switzerland (e.g., Prasuhn, 2011). However, this is not a limitation of our results considering the high variability and uncertainty of erosion measurement methods (García-Ruiz et al., 2015) and that we based the analysis on a comparison between future and present erosion estimates rather than on the absolute values (Li and Fang, 2017).

Furthermore, the bias-corrected ERA5 data could have been used directly as an input to the LEM to simulate the hydromorphological response to the present climate. However, since we simulated climate variables for the future climate using the AWE-GEN weather generator, we had to be consistent and use the model to simulate hourly precipitation, temperature, and wind for the present climate instead of using the ERA5 data directly. The main advantage of using the AWE-GEN model is its ability to ensure the cross-correlation between temperature and precipitation.

We investigated the hydromorphological responses to climate change in a pre-Alpine area using a single catchment. Nonetheless, as this catchment is a representative pre-Alpine catchment, with typical pre-Alpine rain/snow-discharge-erosion interactions, and as the magnitude of climate change is projected to be similar across the region, we think the general findings observed in our study could be applicable to other pre-Alpine catchments as well.

6. Conclusions

We present a framework to study the impact of climate change on sediment erosion and deposition in nivo-pluvial catchments, i.e., where snow processes and their future changes are relevant together with changes in rainfall. Our results demonstrate that the projected changes in the hydromorphological response are characterized by high variability - both temporally (e.g., seasonal changes) and spatially (e.g., within the catchment; elevation-dependent). It highlights the need to simulate future geomorphological changes using a high space-time resolution modeling chain, and the necessity of using spatially varying precipitation and including temperature-driven processes like precipitation partitioning and snowmelt. Moreover, we demonstrate that most of the erosion and sediment transport occur in response to heavy precipitation events, which last only a small fraction of the geomorphic system evolution time. This points to the importance of modeling not only the mean changes in precipitation but also to explicitly consider the intensification of heavy precipitation events in climate change studies.

The results of our numerical experiment imply that more erosion is to be expected at the end of the century over pre-Alpine regions, despite the decrease in precipitation and discharge amounts. The main factors controlling erosion fluxes are the future intensification of heavy precipitation, in combination with catchments becoming more pluvial and less nivo-pluvial dominated. Higher erosion rates are expected in future wet months with equal net precipitation to present but with higher rainfall intensities. The most pronounced changes in erosion processes are foreseen in winter and autumn months, while spring and summer months show respectively a decrease or varying changes in erosion rates in the future. Higher erosion rates are expected at mid-elevations, while a shift from erosion- to deposition-dominated patterns is foreseen in the valleys. Further research is required to quantify the economic (e.g., for the hydropower sector) and ecologic (e.g., river fauna and flora) implications of these changes.

Declaration of competing interest

The authors declare that they have no known competing financial interests or personal relationships that could have appeared to influence the work reported in this paper.

Data availability

Data will be made available on request.

Acknowledgments

TC and NP acknowledge the support of the Swiss National Science Foundation (SNSF), Grant 194649 (“Rainfall and floods in future cities”). The authors thank MeteoSwiss, the Swiss Federal Office for the Environment and WSL for providing the climate, hydrological and snow depth data. The results contain modified Copernicus Climate Change Service information 2020. Neither the European Commission nor ECMWF is responsible for any use that may be made of the Copernicus information or data it contains. The authors also thank Fritz Schlunegger for reviewing our paper and for his constructive suggestions and time.

Appendix A. Supplementary data

Supplementary data to this article can be found online at https://doi.org/10.1016/j.geomorph.2023.108782.

References

Ali, H., Fowler, H.J., Lenderink, G., Lewis, E., Pritchard, D., 2021a. Consistent large-scale response of hourly extreme precipitation to temperature variation over land. Geophys. Res. Lett. 48 https://doi.org/10.1029/2020GL090317 e2020GL090317.

Ali, H., Peleg, N., Fowler, H.J., 2021b. Global scaling of rainfall with dewpoint temperature reveals considerable ocean-land difference. Geophys. Res. Lett. 48 https://doi.org/10.1029/2021GL093798 e2021GL093798.

Alves, M., Nadeau, D.F., Music, B., Anctil, F., Fatichi, S., 2021. Can we replace observed forcing with weather generator in land surface modeling? Insights from long-term

simulations at two contrasting boreal sites. Theor Appl Clilmatol. 145, 215–244. https://doi.org/10.1007/s00704-021-03615-y.
Bates, P.D., Horritt, M.S., Fewtrell, T.J., 2010. A simple inertial formulation of the shallow water equations for efficient two-dimensional flood inundation modelling. J. Hydrol. 387, 33–45. https://doi.org/10.1016/j.jhydrol.2010.03.027.
Battista, G., Molnar, P., Burlando, P., 2020a. Modelling impacts of spatially variable erosion drivers on suspended sediment dynamics. Earth Surface Dynamics. 8, 619–635. https://doi.org/10.5194/esurf-8-619-2020.
Battista, G., Schlunegger, F., Burlando, P., Molnar, P., 2020b. Modelling localized sources of sediment in mountain catchments for provenance studies. Earth Surf. Process. Landf. 45, 3475–3487. https://doi.org/10.1002/ESP.4979.
Battista, G., Schlunegger, F., Burlando, P., Molnar, P., 2022. Sediment supply effects in hydrology-sediment modeling of an alpine basin. Water Resour. Res. 58 https://doi.org/10.1029/2020WR029408 e2020WR029408.
Baudirektion des Kantons Bern, 1988. Emme 2050: Die Sohleneintiefung der Emme macht Sorgen: Die Emme wiederwieder ins Gleichgewicht bringen!.
Bavay, M., Grünewald, T., Lehning, M., 2013. Response of snow cover and runoff to climate change in high Alpine catchments of Eastern Switzerland. Adv. Water Resour. 55, 4–16. https://doi.org/10.1016/j.advwatres.2012.12.009.
Beel, C.R., Lamoureux, S.F., Orwin, J.F., 2018. Fluvial response to a period of hydrometeorological change and landscape disturbance in the Canadian high arctic. Geophys. Res. Lett. 45, 10446–10455. https://doi.org/10.1029/2018GL079660.
Beniston, M., 2012. Is snow in the Alps receding or disappearing? Wiley Interdiscip. Rev. Clim. Chang. 3, 349–358. https://doi.org/10.1002/WCC.179.
Bennett, G.L., Molnar, P., McArdell, B.W., Schlunegger, F., Burlando, P., 2013. Patterns and controls of sediment production, transfer and yield in the Illgraben. Geomorphology. 188, 68–82. https://doi.org/10.1016/j.geomorph.2012.11.029.
Bennett, G.L., Molnar, P., McArdell, B.W., Burlando, P., 2014. A probabilistic sediment cascade model of sediment transfer in the Illgraben. Water Resour. Res. 50, 1225–1244. https://doi.org/10.1002/2013WR013806.
Beven, K.J., Kirkby, M.J., 1979. A Physically Based, Variable Contributing Area Model of Basin Hydrology, 24, pp. 43–69. https://doi.org/10.1080/02626667909491834.
Bilotta, G.S., Brazier, R.E., 2008. Understanding the influence of suspended solids on water quality and aquatic biota. Water Res. 42, 2849–2861. https://doi.org/10.1016/J.WATRES.2008.03.018.
Brock, B.W., Willis, I.C., Sharp, M.J., 2000. Measurement and parameterization of albedo variations at Haut Glacier d'Arolla, Switzerland. Journal of Glaciology. 46, 675–688. https://doi.org/10.3189/172756500781832675.
Carenzo, M., Pellicciotti, F., Rimkus, S., Burlando, P., 2009. Assessing the transferability and robustness of an enhanced temperature-index glacier-melt model. J. Glaciol. 55, 258–274. https://doi.org/10.3189/002214309788608804.
Cavalli, M., Trevisani, S., Comiti, F., Marchi, L., 2013. Geomorphometric assessment of spatial sediment connectivity in small Alpine catchments. Geomorphology. 188, 31–41. https://doi.org/10.1016/J.GEOMORPH.2012.05.007.
CH2018, 2018. CH2018-Climate Scenarios for Switzerland, Technical Report. In: National Centre for Climate Services, Zurich, 271, ISBN 978-3-9525031-4-0.
Chiarle, M., Geertsema, M., Mortara, G., Clague, J.J., 2021. Relations between climate change and mass movement: perspectives from the Canadian Cordillera and the European Alps. Glob Planet Change. 202, 103499 https://doi.org/10.1016/j.gloplacha.2021.103499.
Costa, A., Anghileri, D., Molnar, P., 2018a. Hydroclimatic control on suspended sediment dynamics of a regulated Alpine catchment: a conceptual approach. Hydrol. Earth Syst. Sci. 22, 3421–3434. https://doi.org/10.5194/hess-22-3421-2018.
Costa, A., Molnar, P., Stutenbecker, L., Bakker, M., Silva, T.A., Schlunegger, F., Lane, S. N., Loizeau, J.L., Girardclos, S., 2018b. Temperature signal in suspended sediment export from an Alpine catchment. Hydrol. Earth Syst. Sci. 22, 509–528. https://doi.org/10.5194/hess-22-509-2018.
Coulthard, T.J., Skinner, C.J., 2016. The sensitivity of landscape evolution models to spatial and temporal rainfall resolution. Earth Surf Dynam. 4, 757–771. https://doi.org/10.5194/esurf-4-757-2016.
Coulthard, T.J., Macklin, M.G., Kirkby, M.J., 2002. A cellular model of Holocene upland river basin and alluvial fan evolution. Earth Surf. Process. Landf. 27, 269–288. https://doi.org/10.1002/esp.318.
Coulthard, T.J., Ramirez, J., Fowler, H.J., Glenis, V., 2012. Hydrology and Earth System Sciences using the UKCP09 probabilistic scenarios to model the amplified impact of climate change on drainage basin sediment yield. Hydrol. Earth Syst. Sci. 16, 4401–4416. https://doi.org/10.5194/hess-16-4401-2012.
Coulthard, T.J., Neal, J.C., Bates, P.D., Ramirez, J., de Almeida, G.A.M., Hancock, G.R., 2013. Integrating the LISFLOOD-FP 2D hydrodynamic model with the CAESAR model: implications for modelling landscape evolution. Earth Surf. Process. Landf. 38, 1897–1906. https://doi.org/10.1002/ESP.3478.
Cucchi, M., Weedon, G.P., Amici, A., Bellouin, N., Lange, S., Schmied, H.M., Hersbach, H., Buontempo, C., 2020. WFDE5: bias adjusted ERA5 reanalysis data for impact studies. Earth System Science Data. 12, 2097–2120. https://doi.org/10.5194/essd-12-2097-2020.
Davies-Colley, R.J., Smith, D.G., 2001. Turbidity, suspended sediment, and water clarity: a review. J. Am. Water Resour. Assoc. 37, 1085–1101. https://doi.org/10.1111/J.1752-1688.2001.TB03624.X.
Einstein, H.A., 1950. The Bed-Load Function for Sediment Transportation in Open Channel Flows. In: Technical Bulletin No. 1026. USDA Soil Conservation Service. US Department of Agriculture.
Etter, S., Addor, N., Huss, M., Finger, D., 2017. Climate change impacts on future snow, ice and rain runoff in a Swiss mountain catchment using multi-dataset calibration. J Hydrol Reg Stud. 13, 222–239. https://doi.org/10.1016/j.ejrh.2017.08.005.
Fatichi, S., Ivanov, V.Y., Caporali, E., 2011. Simulation of future climate scenarios with a weather generator. Adv. Water Resour. 34, 448–467. https://doi.org/10.1016/j.advwatres.2010.12.013.
Fatichi, S., Ivanov, V.Y., Paschalis, A., Peleg, N., Molnar, P., Rimkus, S., Kim, J., Burlando, P., Caporali, E., 2016. Uncertainty partition challenges the predictability of vital details of climate change. Earths Future. 4, 240–251. https://doi.org/10.1002/2015EF000336.
Fatichi, S., Peleg, N., Mastrotheodoros, T., Pappas, C., Manoli, G., 2021. An ecohydrological journey of 4500 years reveals a stable but threatened precipitation-groundwater recharge relation around Jerusalem. Sci. Adv. 7, eabe6303. https://doi.org/10.1126/SCIADV.ABE6303.
Feeney, C.J., Chiverrell, R.C., Smith, H.G., Hooke, J.M., Cooper, J.R., 2020. Modelling the decadal dynamics of reach-scale river channel evolution and floodplain turnover in CAESAR-Lisflood. Earth Surf. Process. Landf. 45, 1273–1291. https://doi.org/10.1002/ESP.4804.
Fowler, H.J., Lenderink, G., Prein, A.F., Westra, S., Allan, R.P., Ban, N., Barbero, R., Berg, P., Blenkinsop, S., Do, H.X., Guerreiro, S., Haerter, J.O., Kendon, E.J., Lewis, E., Schaer, C., Sharma, A., Villarini, G., Wasko, C., Zhang, X., 2021. Anthropogenic intensification of short-duration rainfall extremes. Nature Reviews Earth and Environment. 2, 107–122. https://doi.org/10.1038/s43017-020-00128-6.
García-Ruiz, J.M., Beguería, S., Nadal-Romero, E., González-Hidalgo, J.C., Lana-Renault, N., Sanjuán, Y., 2015. A meta-analysis of soil erosion rates across the world. Geomorphology. 239, 160–173. https://doi.org/10.1016/j.geomorph.2015.03.008.
Geitner, C., Mayr, A., Rutzinger, M., Löbmann, M.T., Tonin, R., Zerbe, S., Wellstein, C., Markart, G., Kohl, B., 2021. Shallow erosion on grassland slopes in the European Alps – Geomorphological classification, spatio-temporal analysis, and understanding snow and vegetation impacts. Geomorphology. 373, 107446 https://doi.org/10.1016/J.GEOMORPH.2020.107446.
Gianinetto, M., Aiello, M., Vezzoli, R., Polinelli, F.N., Rulli, M.C., Chiarelli, D.D., Bocchiola, D., Ravazzani, G., Soncini, A., 2020. Future scenarios of soil erosion in the alps under climate change and land cover transformations simulated with automatic machine learning. Climate. 8, 28. https://doi.org/10.3390/cli8020028.
Goudie, A.S., 2006. Global warming and fluvial geomorphology. Geomorphology. 79, 384–394. https://doi.org/10.1016/J.GEOMORPH.2006.06.023.
Hackney, C.R., Darby, S.E., Parsons, D.R., Leyland, J., Best, J.L., Aalto, R., Nicholas, A.P., Houseago, R.C., 2020. River bank instability from unsustainable sand mining in the lower Mekong River. Nat Sustain. 3, 217–225. https://doi.org/10.1038/S41893-019-0455-3.
Hall, D.K., Riggs, G.A., 2021. MODIS/Terra Snow Cover 8-Day L3 Global 500m Grid, Version 61. NASA National Snow and Ice Data Center Distributed Active Archive Center. https://doi.org/10.5067/MODIS/MOD10A2.061.
Hegerl, G.C., Black, E., Allan, R.P., Ingram, W.J., Polson, D., Trenberth, K.E., Chadwick, R.S., Arkin, Beena Balan, Sarojini, P.A., Becker, A., Durack, P.J., Easterling, D., Fowler, H.J., Kendon, J., Huffman, G.J., Liu, C., Marsh, R., Osborn, T. J., Stott, P.A., Vidale, P.-L., Wijffels, S.E., Wilcox, L.J., Willett, K.M., Zhang, X., 2015. Challenges in quantifying changes in the global water. Cycle. 96, 1097–1115. https://doi.org/10.1175/BAMS-D-13-00212.2.
Hersbach, H., Bell, B., Berrisford, P., Biavati, G., Horányi, A., Muñoz Sabater, J., Nicolas, J., Peubey, C., Radu, R., Rozum, I., Schepers, D., Simmons, A., Soci, C., Dee, D., Thépaut, J.-N., 2018. ERA5 Hourly Data on Single Levels From 1959 to Present, Copernicus Climate Change Service (C3S) Climate Data Store (CDS) [data set]. In: URL. https://cds.climate.copernicus.eu/cdsapp#!/dataset/reanalysis-era5-single-levels?tab=overview. accessed 08.04.21.
Hersbach, H., Bell, B., Berrisford, P., Hirahara, S., Horányi, A., Muñoz-Sabater, J., Nicolas, J., Peubey, C., Radu, R., Schepers, D., Simmons, A., Soci, C., Abdalla, S., Abellan, X., Balsamo, G., Bechtold, P., Biavati, G., Bidlot, J., Bonavita, M., de Chiara, G., Dahlgren, P., Dee, D., Diamantakis, M., Dragani, R., Flemming, J., Forbes, R., Fuentes, M., Geer, A., Haimberger, L., Healy, S., Hogan, R.J., Hólm, E., Janisková, M., Keeley, S., Laloyaux, P., Lopez, P., Lupu, C., Radnoti, G., de Rosnay, P., Rozum, I., Vamborg, F., Villaume, S., Thépaut, J.N., 2020. The ERA5 global reanalysis. Q. J. R. Meteorol. Soc. 146, 1999–2049. https://doi.org/10.1002/QJ.3803.
Hirschberg, J., Fatichi, S., Bennett, G.L., McArdell, B.W., Peleg, N., Lane, S.N., Schlunegger, F., Molnar, P., 2021. Climate change impacts on sediment yield and debris-flow activity in an Alpine catchment. J. Geophys. Res. Earth Surf. 126 https://doi.org/10.1029/2020JF005739 e2020JF005739.
Hoober, D., Svoray, T., Cohen, S., 2017. Using a landform evolution model to study ephemeral gullying in agricultural fields: the effects of rainfall patterns on ephemeral gully dynamics. Earth Surf. Process. Landf. 42, 1213–1226. https://doi.org/10.1002/ESP.4090.
Horton, P., 2021. Analogue methods and ERA5: benefits and pitfalls. Int. J. Climatol. 42, 4078–4096. https://doi.org/10.1002/joc.7484.
Huggel, C., Salzmann, N., Allen, S., Caplan-Auerbach, J., Fischer, L., Haeberli, W., Larsen, C., Schneider, D., Wessels, R., 2010. Recent and future warm extreme events and high-mountain slope stability. Philosophical Trans Res Soc A. 368, 2435–2459. https://doi.org/10.1098/rsta.2010.0078.
Huggel, C., Clague, J.J., Korup, O., 2012. Is climate change responsible for changing landslide activity in high mountains? Earth Surf. Process. Landf. 37, 77–91. https://doi.org/10.1002/ESP.2223.
Huss, M., Bookhagen, B., Huggel, C., Jacobsen, D., Bradley, R.S., Clague, J.J., Vuille, M., Buytaert, W., Cayan, D.R., Greenwood, G., Mark, B.G., Milner, A.M., Weingartner, R., Winder, M., 2017. Toward mountains without permanent snow and ice. Earths Future. 5, 418–435. https://doi.org/10.1002/2016EF000514.
Iida, T., Kajihara, A., Okubo, H., Okajima, K., 2012. Effect of seasonal snow cover on suspended sediment runoff in a mountainous catchment. J. Hydrol. 428–429, 116–128. https://doi.org/10.1016/j.jhydrol.2012.01.029.

IPCC, 2022. Impacts of 1.5°C Global Warming on Natural and Human Systems. In: Global Warming of 1.5°C: IPCC Special Report on Impacts of Global Warming of 1.5°C above Pre-Industrial Levels in Context of Strengthening Response to Climate Change, Sustainable Development, and Efforts to Eradicate Poverty. Cambridge University Press, pp. 175–312. https://doi.org/10.1017/9781009157940.005.

Lane, S.N., Tayefi, V., Reid, S.C., Yu, D., Hardy, R.J., 2007. Interactions between sediment delivery, channel change, climate change and flood risk in a temperate upland environment. Earth Surf. Process. Landf. 32, 429–446. https://doi.org/10.1002/ESP.1404.

Lenderink, G., van Meijgaard, E., 2008. Increase in Hourly Precipitation Extremes Beyond Expectations From Temperature Changes, 1, pp. 511–514. https://doi.org/10.1038/ngeo262.

Lewis, T., Lamoureux, S.F., 2010. Twenty-first century discharge and sediment yield predictions in a small high Arctic watershed. Glob Planet Change. 71, 27–41. https://doi.org/10.1016/j.gloplacha.2009.12.006.

Li, D., Li, Z., Zhou, Y., Lu, X., 2020. Substantial increases in the water and sediment fluxes in the headwater region of the Tibetan Plateau in response to global warming. Geophys. Res. Lett. 47 https://doi.org/10.1029/2020GL087745 e2020GL087745.

Li, Z., Fang, H., 2017. Modeling the impact of climate change on watershed discharge and sediment yield in the black soil region, northeastern China. Geomorphology. 293, 255–271. https://doi.org/10.1016/J.GEOMORPH.2017.06.005.

Mann, H.B., Whitney, D.R., 1947. On a test of whether one of two random variables is stochastically larger than the other. Ann. Math. Stat. 18, 50–60. https://doi.org/10.1214/aoms/1177730491.

Marty, C., 2008. Regime shift of snow days in Switzerland. Geophys. Res. Lett. 35, L12501. https://doi.org/10.1029/2008GL033998.

Meißl, G., Formayer, H., Klebinder, K., Kerl, F., Schöberl, F., Geitner, C., Markart, G., Leidinger, D., Bronstert, A., 2017. Climate change effects on hydrological system conditions influencing generation of storm runoff in small Alpine catchments. Hydrol. Process. 31, 1314–1330. https://doi.org/10.1002/HYP.11104.

Meusburger, K., Steel, A., Panagos, P., Montanarella, L., Alewell, C., 2012. Spatial and temporal variability of rainfall erosivity factor for Switzerland. Hydrol. Earth Syst. Sci. 16, 167–177. https://doi.org/10.5194/HESS-16-167-2012.

Meusburger, K., Leitinger, G., Mabit, L., Mueller, M.H., Walter, A., Alewell, C., 2014. Soil erosion by snow gliding - a first quantification attempt in a subalpine area in Switzerland. Hydrol. Earth Syst. Sci. 18, 3763–3775. https://doi.org/10.5194/hess-18-3763-2014.

Meyer-Peter, E., Müller, R., 1948. Formulas for bedload transport. In: 2nd Meeting of the International Association for Hydraulic Structures Research, Stockholm, Sweden, pp. 1–26.

Micheletti, N., Lane, S.N., 2016. Water yield and sediment export in small, partially glaciated Alpine watersheds in a warming climate. Water Resour. Res. 52, 4924–4943. https://doi.org/10.1002/2016WR018774.

Micheletti, N., Lambiel, C., Lane, S.N., 2015. Investigating decadal-scale geomorphic dynamics in an alpine mountain setting. Journal of Geophysical Research: Earth Surface. 120, 2155–2175. https://doi.org/10.1002/2015JF003656.

Molnar, P., Fatichi, S., Gaál, L., Szolgay, J., Burlando, P., 2015. Storm type effects on super Clausius-Clapeyron scaling of intense rainstorm properties with air temperature. Hydrol. Earth Syst. Sci. 19, 1753–1766. https://doi.org/10.5194/hess-19-1753-2015.

Moraga, J.S., Peleg, N., Fatichi, S., Molnar, P., Burlando, P., 2021. Revealing the impacts of climate change on mountainous catchments through high-resolution modelling. J. Hydrol. 603, 126806 https://doi.org/10.1016/j.jhydrol.2021.126806.

Muelchi, R., Rössler, O., Schwanbeck, J., Weingartner, R., Martius, O., 2021a. River runoff in Switzerland in a changing climate-runoff regime changes and their time of emergence. Hydrol. Earth Syst. Sci. 25, 3071–3086. https://doi.org/10.5194/hess-25-3071-2021.

Muelchi, R., Rössler, O., Schwanbeck, J., Weingartner, R., Martius, O., 2021b. An ensemble of daily simulated runoff data (1981–2099) under climate change conditions for 93 catchments in Switzerland (Hydro-CH2018-runoff ensemble). Geosci Data J. 9, 46–57. https://doi.org/10.1002/gdj3.117.

Mukundan, R., Pradhanang, S.M., Schneiderman, E.M., Pierson, D.C., Anandhi, A., Zion, M.S., Matonse, A.H., Lounsbury, D.G., Steenhuis, T.S., 2013. Suspended sediment source areas and future climate impact on soil erosion and sediment yield in a New York City water supply watershed, USA. Geomorphology. 183, 110–119. https://doi.org/10.1016/J.GEOMORPH.2012.06.021.

Nash, E., Sutcliffe, V., 1970. River flow forecasting through conceptual models. Part I – a discussion of principles. J. Hydrol. 10, 282–290. https://doi.org/10.1016/0022-1694(70)90255-6.

Palazón, L., Navas, A., 2016. Land use sediment production response under different climatic conditions in an alpine–prealpine catchment. Catena. 137, 244–255. https://doi.org/10.1016/j.catena.2015.09.025.

Paschalis, A., Molnar, P., Fatichi, S., Burlando, P., 2013. A stochastic model for high-resolution space-time precipitation simulation. Water Resour. Res. 49, 8400–8417. https://doi.org/10.1002/2013WR014437.

Peleg, N., Molnar, P., Burlando, P., Fatichi, S., 2019. Exploring stochastic climate uncertainty in space and time using a gridded hourly weather generator. J. Hydrol. 571, 627–641. https://doi.org/10.1016/j.jhydrol.2019.02.010.

Peleg, N., Skinner, C., Fatichi, S., Molnar, P., 2020. Temperature effects on the spatial structure of heavy rainfall modify catchment hydro-morphological response. Earth Surface Dynamics. 8, 17–36. https://doi.org/10.5194/esurf-8-17-2020.

Peleg, N., Skinner, C., Ramirez, J.A., Molnar, P., 2021. Rainfall spatial-heterogeneity accelerates landscape evolution processes. Geomorphology. 390, 107863 https://doi.org/10.1016/j.geomorph.2021.107863.

Peleg, N., Ban, N., Gibson, M.J., Chen, A.S., Paschalis, A., Burlando, P., Leitão, J.P., 2022. Mapping storm spatial profiles for flood impact assessments. Adv. Water Resour. 166, 104258 https://doi.org/10.1016/J.ADVWATRES.2022.104258.

Piani, C., Haerter, J.O., Coppola, E., 2010. Statistical bias correction for daily precipitation in regional climate models over Europe. Theor. Appl. Climatol. 99, 187–192. https://doi.org/10.1007/S00704-009-0134-9.

Poeppl, R.E., Coulthard, T., Keesstra, S.D., Keiler, M., 2019. Modeling the impact of dam removal on channel evolution and sediment delivery in a multiple dam setting. International Journal of Sediment Research. 34, 537–549. https://doi.org/10.1016/J.IJSRC.2019.06.001.

Prasuhn, V., 2011. Soil erosion in the Swiss midlands: results of a 10-year field survey. Geomorphology. 126, 32–41. https://doi.org/10.1016/J.GEOMORPH.2010.10.023.

Ragettli, S., Pellicciotti, F., 2012. Calibration of a physically based, spatially distributed hydrological model in a glacierized basin: on the use of knowledge from glaciometeorological processes to constrain model parameters. Water Resour. Res. 48, W03509. https://doi.org/10.1029/2011WR010559.

Ramirez, J.A., Zischg, A.P., Schürmann, S., Zimmermann, M., Weingartner, R., Coulthard, T., Keiler, M., 2020. Modeling the geomorphic response to early river engineering works using CAESAR-Lisflood. Anthropocene. 32, 100266 https://doi.org/10.1016/J.ANCENE.2020.100266.

Ramirez, J.A., Mertin, M., Peleg, N., Horton, P., Skinner, C., Zimmermann, M., Keiler, M., 2022. Modelling the long-term geomorphic response to check dam failures in an alpine channel with CAESAR-Lisflood. International Journal of Sediment Research 37, 687–700. https://doi.org/10.1016/J.IJSRC.2022.04.005.

Reynard, E., Lambiel, C., Lane, S.N., 2012. Climate change and integrated analysis of mountain geomorphological systems. Geogr Helv. 67, 5–14. https://doi.org/10.5194/gh-67-5-2012.

Ruiz-Villanueva, V., Stoffel, M., Bussi, G., Francés, F., Bréthaut, C., 2015. Climate change impacts on discharges of the Rhone River in Lyon by the end of the twenty-first century: model results and implications. Reg. Environ. Chang. 15, 505–515. https://doi.org/10.1007/s10113-014-0707-8.

Scherrer, S.C., Appenzeller, C., Laternser, M., 2004. Trends in Swiss Alpine snow days: the role of local- and large-scale climate variability. Geophys. Res. Lett. 31, L13215. https://doi.org/10.1029/2004GL020255.

Skinner, C.J., Coulthard, T.J., Schwanghart, W., Van De Wiel, M.J., Hancock, G., 2018. Global sensitivity analysis of parameter uncertainty in landscape evolution models. Geosci. Model Dev. 11, 4873–4888. https://doi.org/10.5194/gmd-11-4873-2018.

Skinner, C.J., Peleg, N., Quinn, N., Coulthard, T.J., Molnar, P., Freer, J., 2020. The impact of different rainfall products on landscape modelling simulations. Earth Surf. Process. Landf. 45, 2512–2523. https://doi.org/10.1002/esp.4894.

Slosson, J.R., Kelleher, C., Hoke, G.D., 2021. Contrasting impacts of a hotter and drier future on streamflow and catchment scale sediment flux in the High Andes. J. Geophys. Res. Earth Surf. 126 https://doi.org/10.1029/2021JF006182 e2021JF006182.

Stanzel, P., Haberl, U., Nachtnebel, H.P., 2008. Modelling snow accumulation and snow melt in a continuous hydrological model for real-time flood forecasting. IOP Conf Ser Earth Environ Sci. 4, 012016 https://doi.org/10.1088/1755-1307/4/1/012016.

Trenberth, K.E., Dai, A., Rasmussen, R.M., Parsons, D.B., 2003. The changing character of Precipitation. Bull. Am. Meteorol. Soc. 84, 1205–1218. https://doi.org/10.1175/BAMS-84-9-1205.

Viviroli, D., Dürr, H.H., Messerli, B., Meybeck, M., Weingartner, R., 2007. Mountains of the world, water towers for humanity: typology, mapping, and global significance. Water Resour. Res. 43, W07447. https://doi.org/10.1029/2006WR005653.

Welsh, K.E., Dearing, J.A., Chiverrell, R.C., Coulthard, T.J., 2009. Testing a cellular modelling approach to simulating late-Holocene sediment and water transfer from catchment to lake in the French Alps since 1826. Holocene 19, 785–798. https://doi.org/10.1177/0959683609105303.

van de Wiel, M.J., Coulthard, T.J., Macklin, M.G., Lewin, J., 2007. Embedding reach-scale fluvial dynamics within the CAESAR cellular automaton landscape evolution model. Geomorphology. 90, 283–301. https://doi.org/10.1016/J.GEOMORPH.2006.10.024.

Wilcock, P.R., Crowe, J.C., 2003. Surface-based Transport Model for Mixed-size Sediment. J. Hydraul. Eng. 129, 120–128. https://doi.org/10.1061/(ASCE)0733-9429(2003)129:2(120).

WMO, 2018. Guide to Climatological Practices, WMO-No. 100. Geneva.

Yin, J., Guo, S., Gu, L., Zeng, Z., Liu, D., Chen, J., Shen, Y., Xu, C.Y., 2021. Blending multi-satellite, atmospheric reanalysis and gauge precipitation products to facilitate hydrological modelling. J. Hydrol. 593, 125878 https://doi.org/10.1016/j.jhydrol.2020.125878.

Zappone, A., Kissling, E., 2021. SAPHYR: Swiss Atlas of Physical Properties of Rocks: the continental crust in a database. Swiss J. Geosci. 114, 13. https://doi.org/10.1186/s00015-021-00389-3.

Ziliani, L., Surian, N., Botter, G., Mao, L., 2020. Assessment of the geomorphic effectiveness of controlled floods in a braided river using a reduced-complexity numerical model. Hydrol. Earth Syst. Sci. 24, 3229–3250. https://doi.org/10.5194/HESS-24-3229-2020.